Spectrochimica Acta Part A: Molecular and Biomolecular Spectroscopy 109 (2013) 179–185

Contents lists available at SciVerse ScienceDirect

Spectrochimica Acta Part A: Molecular and Biomolecular Spectroscopy

journal homepage: www.elsevier.com/locate/saa

Synthesis, crystal structure and photoluminescence of phosphorescent copper (I) complexes containing hole-transporting carbazoly moiety

Tianzhi Yu [a,*], Haifang Chai [a,b], Yuling Zhao [b], Chengcheng Zhang [a,b], Peng Liu [a,b], Duowang Fan [a]

[a] Key Laboratory of Opto-Electronic Technology and Intelligent Control, Ministry of Education, Lanzhou Jiaotong University, Lanzhou 730070, China
[b] School of Chemical and Biological Engineering, Lanzhou Jiaotong University, Lanzhou 730070, China

HIGHLIGHTS

- One new ligand **L** and two new Cu(I) complexes based on 2-(2′-pyridyl) benzimidazolyl derivative ligand were synthesized.
- Their structures were characterized by elemental analysis, ^{1}H NMR, FT-IR spectra and single crystal X-ray diffraction.
- The complexes exhibit strong orange emissions in solid state.

GRAPHICAL ABSTRACT

One new ligand **L** and two new copper (I) complexes based on 2-(2′-pyridyl)benzimidazolyl derivative ligand containing hole-transporting carbazole, L, [Cu(L)(DPEphos)](BF_4) and [Cu(L)(PPh_3)$_2$](BF_4), were synthesized and characterized. Their structures have been characterized by X-ray crystallography. The complexes exhibit strong orange emissions.

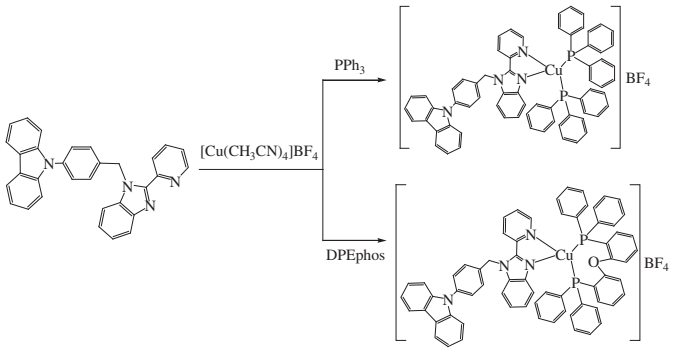

ARTICLE INFO

Article history:
Received 12 September 2012
Received in revised form 1 November 2012
Accepted 5 November 2012
Available online 8 March 2013

Keywords:
Copper (I) complex
Crystal structure
Benzimidazolyl derivative
Photoluminescence

ABSTRACT

Two new mononuclear Cu(I) complexes based on 2-(2′-pyridyl)benzimidazolyl derivative ligand containing hole-transporting carbazole (**L**), [Cu(L)(DPEphos)](BF_4) and [Cu(L)(PPh_3)$_2$](BF_4), where **L** = (4-(9*H*-carbazol-9-yl)phenyl)methyl-2-(2′-pyridyl)benzimidazole; DPEphos = bis[2-(diphenylphosphino)phenyl] ether and PPh_3 = triphenylphosphine, have been synthesized and characterized on the basis of elemental analysis, ^{1}H NMR and FT-IR spectra. The structures of the ligand **L** and the Cu(I) complexes were characterized by single crystal X-ray diffraction. The results reveal that in the Cu(I) complexes the central Cu(I) ions assume the irregular distorted tetrahedral geometry and are tetra-coordinated by the two nitrogen atoms from **L** ligand and two phosphorus atoms from ancillary ligands. The photophysical properties of the complexes were examined by using UV–vis, photoluminescence spectroscopic analysis. The complexes exhibit weak MLCT absorption bands ranging from 360 to 480 nm, and display strong orange phosphorescence in the solid states at room temperature, which is completely quenched in solutions.

Introduction

Recently, the synthesis of luminescent transition metal complexes was extensively investigated due to their wide range of applications. The luminescent transition metal complexes generally used as emitters in organic light-emitting diodes (OLEDs) [1–3] and in light emitting electro-chemical cells (LEECs) [4,5], as chemo- and biosensors [6,7], and as lumophores for cell imagings [8,9]. By choosing appropriate metal ions and organic building blocks, it is possible to control and coordinate the structures and the photonic properties of metal complexes.

* Corresponding author. Tel.: +86 931 4956935; fax: +86 931 4938756.
E-mail address: yutianzhi@hotmail.com (T. Yu).

1386-1425/$ - see front matter © 2013 Elsevier B.V. All rights reserved.
http://dx.doi.org/10.1016/j.saa.2012.11.022

OLEDs doped phosphorescent metal complexes, both singlet and triplet excitons can be harvested for light owing to intersystem crossing of the singlet excited states to the triplet states, can exhibit high external quantum efficiency (EQE) of >20% [10–12], which is much higher than the theoretical limit of 5% for fluorescent OLEDs. In the phosphorescent metal complexes, cyclometalated iridium complexes are the most valuable emitting materials due to their high quantum efficiency, brightness, color diversity and short excited-state lifetime.

Although Cu(I) complexes have relatively low quantum yields as compared with the rare and noble metal complexes, phosphorescent Cu(I) complexes have attracted much attention as a new class of optoelectronic materials in chemical sensors, probes of biological systems and OLEDs because of their advantages of less toxic, low cost, stable supply of copper metal and environmental friendliness [13–18]. Recently, some OLEDs doped phosphorescent Cu(I) complexes realized efficiencies comparable to those doped Ir(III) complexes [17,19]. Wada and co-workers [19] reported a high efficiency OLEDs containing [Cu(QuTz)(DPEphos)]BF4 (QuTz = 2-(5-tetrazolyl)quinoline, DPEphos = bis(2-(diphenylphosphino) phenyl)ether) which displayed efficient luminescence with EQE = 7.4%. The OLEDs using a highly emissive dinuclear Cu(I) complex $[(PNP\text{-}^{t}Bu)Cu]_2$ ($PNP\text{-}^{t}Bu^{-}$ = bis(2-diisobutylphosphino-4-*tert*-butylphenyl)amido) exhibited a maximum external quantum efficiency of 16.1% [17]. Hashimoto et al. [16] reported on the photophysical properties of a series of highly emissive three-coordinate Cu(I) complexes containing a chelating bisphosphine ligand (dtpb = 1,2-bis(*o*-ditolylphosphino)benzene), and the best OLED devices with (dtpb)CuBr as dopant exhibited bright green luminescence with a current efficiency of 65.3 cd/A and a maximum external quantum efficiency of 21.3%. These examples were indicated that the inexpensive and non-toxic Cu(I) complexes could be used as promising candidates for OLEDs applications.

Herein two new mononuclear Cu(I) complexes containing hole-transporting carbazoly moiety, $[Cu(L)(DPEphos)](BF_4)$ and $[Cu(L)(PPh_3)_2](BF_4)$ (L = (4-(9*H*-carbazol-9-yl)phenyl)methyl-2-(2′-pyridyl)benzimidazole), were synthesized and characterized by elemental analysis, ^1H NMR and single crystal X-ray crystallography. The photophysical properties of the complexes were examined by using UV–vis, photoluminescence spectroscopies analysis.

Experimental

Materials and methods

$Cu(BF_4)_2{\cdot}6H_2O$, bis[2-(diphenylphosphino)phenyl]ether (DPEphos) and carbazole were purchased from Aldrich. 2-(2-Pyridyl)benzimidazole and triphenylphosphine (PPh_3) were obtained from Acros Organics. *p*-Bromobenzaldehyde was bought from Aladdin Chemistry Co., Ltd. Tri-*tert*-butylphosphine was purchased from Puyang Huicheng Electronic Materials Co., Ltd. Sodium borohydride was obtained from Shanghai Zhongqin chemical reagent Co. Ltd. Copper power was from Shenyang Keda Chemical Reagent Factory (China). All other chemicals were analytical grade reagent.

$[Cu(NCCH_3)_4](BF_4)$ was obtained by reaction of $Cu(BF_4)_2{\cdot}6H_2O$ and copper power in acetonitrile according to the method reported by Kubas [20].

IR spectra (400–4000 cm^{-1}) were measured on a Shimadzu IRPrestige-21 FT-IR spectrophotometer. ^1H NMR spectra were obtained on Unity Varian-500 MHz. C, H, and N analyses were obtained using an Elemental Vario-EL automatic elemental analysis instrument. UV–vis absorption and photoluminescent spectra were recorded on a Shimadzu UV-2550 spectrometer and on a Perkin–Elmer LS-55 spectrometer, respectively. Melting points were measured by using an X-4 microscopic melting point apparatus made in Beijing Taike Instrument Limited Company, and the thermometer was uncorrected.

Synthesis and characterization of (4-(9H-carbazol-9-yl)phenyl)methyl-2-(2′-pyridyl)benz-imidazole (L)

The synthetic routes of ligand **L** are shown in Scheme 1.

4-(9*H*-carbazol-9-yl)benzaldehyde: 0.090 g (3.7 mol%) of $P(t\text{-}Bu)_3$ and 0.035 g (1.3 mol%) $Pd(OAC)_2$ were added to 80 mL degassed toluene, followed by 2.5 g (0.0135 mol) of 4-bromobenzaldehyde and 2.000 g (0.0120 mol) of 9*H*-carbazole and 4.150 g (0.0300 mol) anhydrous K_2CO_3. The reaction mixture was heated to 115 °C for 24 h. The solvent was removed under vacuum, and 150 mL CH_2Cl_2 was added. The material was washed with 2 × 50 mL 20% NaOH, washed with 1 × 50 mL brine, and dried with anhydrous $MgSO_4$. The solvent was removed under vacuum, and the residue was purified by column chromatography on silica gel using ethyl acetate/petroleum ether (1:20, v/v) as the eluent to give 4-(9*H*-carbazol-9-yl)benzaldehyde as white powder (2.65 g, 81.7%). m.p.: 156–158 °C. ^1H NMR ($CDCl_3$, δ, ppm): 10.13 (s, 1H, —CHO), 8.16 (dd, J = 8.5 Hz, 4H), 7.81 (d, J = 8.0 Hz, 2H), 7.52 (d, J = 8.0 Hz, 2H), 7.45 (t, J = 7.6 Hz, 2H), 7.34 (t, J = 8.0 Hz, 2H).

(4-(9*H*-carbazol-9-yl)phenyl)methanol: 2.200 g (0.008 mol) of 4-(9*H*-carbazol-9-yl)benzaldehyde, 0.153 g (0.5 eq, 0.004 mol) of $NaBH_4$, and 1.2 mL 20% NaOH were added to a mixture of 37 mL THF and 37 mL MeOH. The solution was stirred for 16 h at room temperature. The reaction mixture was poured into 100 mL H_2O, and then neutralized with 3 M HCl. The solution was extracted with CH_2Cl_2 (3 × 50 mL) and then dried over anhydrous $MgSO_4$. After filtering, the solvent was removed under vacuum, and the residue was taken up in 10 mL hot CH_2Cl_2. Hexanes were added dropwise until (4-(9*H*-carbazol-9-yl)phenyl)methanol precipitated out. 1.83 g of fine needles of the alcohol product was obtained. The total yield of (4-(9*H*-carbazol-9-yl)phenyl)methanol was 1.83 g (82.57%). m.p.: 120–122 °C. ^1H NMR ($CDCl_3$, δ, ppm): 8.15 (d, J = 7.4 Hz, 2H), 7.63 (d, J = 8.8 Hz, 2H), 7.58 (d, J = 8.4 Hz, 2H), 7.42 (t, J = 7.4 Hz, 2H), 7.32 (d, J = 8.2 Hz, 2H), 7.29 (t, J = 7.4 Hz, 2H), 4.85 (d, J = 5.6 Hz, 2H), 1.81 (t, J = 5.6 Hz, 1H).

9-(4-(bromomethyl)phenyl)-9*H*-carbazole: 2.400 g (0.0088 mol) of (4-(9*H*-carbazol-9-yl)phenyl)methanol was added to 60 mL of dry THF under N_2 and cooled to 0 °C. 0.42 mL (0.5 eq, 0.0044 mol) PBr_3 was added dropwise and then stirred for 16 h at room temperature. The mixture was neutralized with $NaHCO_3$, and then extracted with CH_2Cl_2 (3 × 50 mL). The organic phase was washed with 2 × 50 mL brine and dried over anhydrous $MgSO_4$. The solvent was removed under vacuum, leaving an orange-brown solid. The crude was not purified and directly used for subsequent preparation of the ligand **L**.

(4-(9*H*-carbazol-9-yl)phenyl)methyl-2-(2′-pyridyl) benzimidazole (L): Under N_2, solid NaH (60% dispersed in mineral oil, 0.120 g) and 2-(2-pyridyl)benzimidazole (0.680 g, 0.0035 mol) in 20 mL of anhydrous DMF was stirred at 80 °C for 2 h. The resulting solution was cooled to room temperature and 9-(4-(bromomethyl)penyl)-9*H*-carbazole (1.400 g, 0.0042 mol) was added. The mixed solution was stirred at 80 °C for 36 h. After completing, the reaction mixture was poured into 100 mL of cool water, and was extracted with dichloromethane (3 × 50 mL). The organic phase was washed with water and dried over anhydrous $MgSO_4$. After removal of solvent, the residue was purified by column chromatography using ethyl acetate/petroleum ether (1: 4, v/v) as the eluent to give a white powder. Yield: 81%. m.p.:186–188 °C. IR (KBr pellet cm^{-1}): 3041 (Aryl-CH), 2931 (—CH_2—), 1614, 1456, 1328, 1150, 750. ^1H NMR($CDCl_3$, δ, ppm): 8.70 (d, 1H, J = 7.4 Hz, Aryl-H), 8.50 (d, 1H, J = 8.0 Hz, Aryl-H), 8.11 (d, 2H, J = 7.6 Hz, Aryl-H), 7.92–7.86 (m, 2H, Aryl-H), 7.48–7.41 (m, 5H, Aryl-H), 7.38–7.33 (m, 7H, Aryl-H), 7.25 (t, 2H, J = 8.8 Hz, Aryl-H), 6.32 (s,

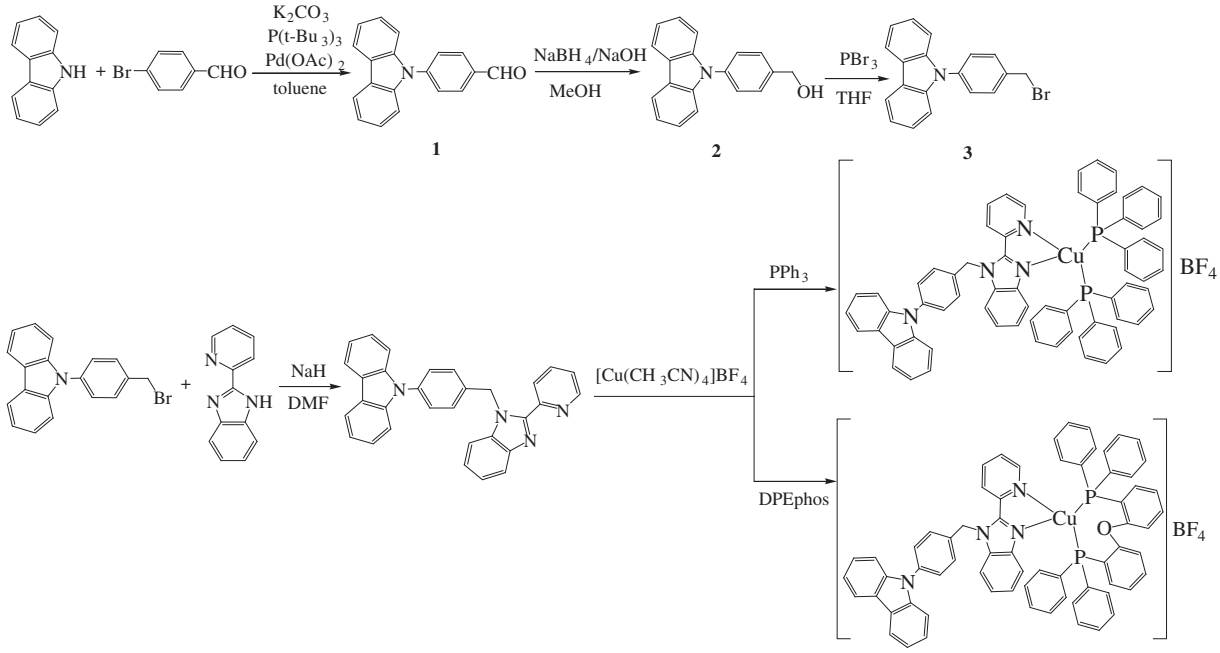

Scheme 1. Synthetic routines to the ligand (**L**) and the Cu (I) complexes.

2H, N—CH_2—Ar). Anal. Calc. for $C_{31}H_{22}N_4$ (%): C, 82.64; H, 4.92; N, 12.44. Found: C, 82.38; H, 5.01; N, 12.52.

Synthesis and characterization of [Cu(L)(DPEphos)](BF_4) and [Cu(L)(PPh_3)$_2$](BF_4)

[Cu(L)(DPEphos)](BF_4) and [Cu(L)(PPh_3)$_2$](BF_4) were synthesized by following procedures described in the literatures [21,22]. All manipulations were performed under a nitrogen atmosphere.

A mixture of [Cu($NCCH_3$)$_4$](BF_4) (1.0 mmol) and PPh_3 (2.0 mmol) or DPEphos (1.0 mmol) in anhydrous dichloromethane (10 mL) was stirred at room temperature for 1 h. (4-(9*H*-carbazol-9-yl)phenyl)methyl-2-(2′-pyridyl)benzimidazole (1.0 mmol) in dichloromethane solution was added to the reaction mixture dropwise and stirring was continued for 12 h at room temperature to result in a clear yellow solution. The reaction mixture was concentrated to 5 mL, then hexane (15 mL) was then introduced to afford a yellow precipitate. The crude product was crystallized from toluene/hexane at ambient temperature to give air-stable, bright yellow crystals.

[Cu(L)(DPEphos)](BF_4): Anal. Calc. for $C_{67}H_{50}N_4OP_2CuBF_4$ (%): C, 70.62; H, 4.42; N, 4.92. Found: C, 70.51; H, 4.38; N, 5.03. ^{1}H NMR($CDCl_3$, δ, ppm): 8.25 (d, 1H, J = 4.8 Hz, Aryl-H), 8.12 (t, 3H, J = 8.0 Hz, Aryl-H), 8.06 (t, 1H, J = 7.6 Hz, Aryl-H), 7.54 (d, 2H, J = 8.4 Hz, Aryl-H), 7.49 (d, 2H, J = 8.8 Hz, Aryl-H), 7.43 (d, 2H, Aryl-H), 7.40–7.35 (m, 5H, Aryl-H), 7.30–7.23 (m, 14H, Aryl-H), 7.20–7.11 (m, 8H, Aryl-H), 7.00 (q, 5H, Aryl-H), 6.93–6.89 (m, 5H, Aryl-H), 6.04 (s, 2H, —CH_2—).

[Cu(L)(PPh_3)$_2$](BF_4): Anal. Calc. for $C_{67}H_{52}N_4P_2CuBF_4$ (%): C, 71.50; H, 4.66; N, 4.98. Found: C, 71.64; H, 4.58; N, 5.06. ^{1}H NMR($CDCl_3$, δ, ppm): 8.27 (d, 1H, J = 8.4 Hz, Aryl-H), 8.22 (d, 1H, J = 5.2 Hz, Aryl-H), 8.13 (q, 3H, J = 7.6 Hz, Aryl-H), 7.59 (d, 1H, J = 8.8 Hz, Aryl-H), 7.50 (d, 2H, J = 8.8 Hz, Aryl-H), 7.45 (t, 1H, J = 8.8 Hz, Aryl-H), 7.38–7.31 (m, 14H, Aryl-H), 7.28–7.25 (m, 5H, Aryl-H), 7.18 (t, 12H, J = 8.0 Hz, Aryl-H), 7.10 (d, 10H, J = 8.0 Hz, Aryl-H), 6.14 (s, 2H, —CH_2—).

Crystallography

The diffraction data were collected with a Bruker Smart Apex CCD area detector with graphite-monochromatized Mo Kα radiation (λ = 0.71073 Å) at 188(2) or 185(2) K. The structure was solved by using the program SHELXL and Fourier difference techniques, and refined by full-matrix least-squares method on F^2. All hydrogen atoms were added theoretically.

Results and discussion

*Syntheses of the ligand **L** and the Cu(I) complexes*

The ligand **L** was prepared in good to excellent yield (81%) in four straightforward steps (Scheme 1), in which the key intermediate **3**, 9-(4-(bromomethyl)phenyl)-9*H*-carbazole, was synthesized using the procedure in the literature [23]. Originally, we synthesized the intermediate **3** by the radical bromination of 9-*p*-tolylcarbazole according to the methods reported by Rajakumar et al. [24] and Xu [25]. Rajakumar and co-workers [24] reported the intermediate **3** was obtained in 84% yield by bromination of 9-*p*-tolylcarbazole, but under the same reaction condition we found 3-bromo-9-p-tolyl-9*H*-carbazole was the main product rather than the intermediate **3**, the yield of the intermediate **3** was very low. The main product 3-bromo-9-p-tolyl-9*H*-carbazole was confirmed by ^{1}H NMR, FT-IR and X-ray single crystal analysis. This experimental result was corroborated by the literature [26].

The ligand **L** was obtained by reaction of the intermediate **3** with 2-(2-pyridyl)benzimidazole in the presence of NaH as a base. The ligand **L** was fairly soluble in most common solvents, such as MeOH, CH_2Cl_2, $CHCl_3$ and EtOAc. The ligand **L** was fully characterized by elemental analysis, ^{1}H NMR, FT-IR and X-ray single crystal analysis.

The Cu(I) complexes [Cu(L)(DPEphos)](BF_4) and [Cu(L)(PPh_3)$_2$](BF_4) were obtained by reaction of [Cu($NCCH_3$)$_4$](BF_4) with **L** and different ancillary phosphoric ligands (PPh_3 and DPEphos) in

anhydrous dichloromethane. The Cu(I) complexes were also examined by elemental analysis, ^{1}H NMR, FT-IR and X-ray single crystal analysis.

*X-ray crystal structure of the ligand **L***

Suitable crystal of the ligand **L** was obtained by evaporation of ethyl acetate solution. The crystallographic data of **L** is shown in Table 1. The selected bond lengths and bond angles of **L** are listed in Table 2. The crystal structure and packing diagram of **L** are given in Fig. 1

The crystal of **L** belongs to the monoclinic space group $P2(1)/c$, $a = 9.4419(8)$ Å, $b = 33.1510(3)$ Å, $c = 7.7622(6)$ Å, $\alpha = \gamma = 90°$, $\beta = 101.9560(10)°$, $U = 2376.9(3)$ Å^3, $Z = 4$, $D_c = 1.259$ g cm^{-3}, $\mu = 0.075$ mm^{-1}. As shown in Fig. 1a, we can see that the pyridyl group and benzimidazole ring of 2-(2-pyridyl)benzimidazole moiety is nearly in a plane, the dihedral angel of them is 0.55°. Otherwise, it is remarkable that carbazole ring, phenyl group and 2-(2-pyridyl)benzimidazole skeleton are not in a coplane. The dihedral angel of carbazole ring and phenyl group is 62.80°, and the dihedral angel of phenyl group and 2-(2-pyridyl)benzimidazole skeleton is 84.18°, and the dihedral angel of carbazole ring and 2-(2-pyridyl)benzimidazole skeleton is 78.18°. From the packing diagram of **L** (Fig. 1b), it is shown that the carbazole group prevents the formation of a regular stacking arrangement of the **L** molecules along *b*-axis, but there are weak intermolecular π–π interactions between the 2-(2-pyridyl)benzimidazole skeletons of two adjacent molecules along *a*-axis in crystal lattices, the interplanar distance of the 2-(2-pyridyl)benzimidazole skeletons is approximately 3.68 Å. This intermolecular π–π interaction causes two adjacent molecules to form a zig-zag chain along *b*-axis.

X-ray crystal structures of the Cu(I) complexes

Suitable crystals of the Cu(I) complexes were obtained by the vapor diffusion of diethyl ether into the acetonitrile solutions of

Table 2
Selected interatomic distances (Å) and angles (°) of **L** and the Cu(I) complexes.

Ligand **L**			
C(1)—N(1)	1.415(3)	C(2)—C(1)—N(1)	131.8(3)
C(6)—N(2)	1.433(3)	C(6)—C(1)—N(1)	105.3(2)
C(7)—N(2)	1.285(3)	C(5)—C(6)—N(2)	128.5(2)
C(7)—N(1)	1.357(3)	C(1)—C(6)—N(2)	110.5(2)
C(8)—N(3)	1.344(3)	N(1)—C(7)—N(2)	116.1(2)
C(12)—N(3)	1.328(4)	N(2)—C(7)—C(8)	119.3(2)
C(13)—N(1)	1.464(3)	N(1)—C(7)—C(8)	124.6(2)
C(17)—N(4)	1.435(3)	C(8)—N(3)—C(12)	117.0(2)
C(20)—N(4)	1.390(3)	N(3)—C(8)—C(7)	119.0(2)
C(30)—N(4)	1.395(3)	N(3)—C(8)—C(9)	121.3(2)
		N(3)—C(12)—C(11)	124.9(3)
		N(1)—C(13)—C(14)	112.07(16)
		N(4)—C(17)—C(16)	120.81(19)
		N(4)—C(17)—C(18)	119.58(19)
		C(17)—N(4)—C(20)	125.94(19)
		C(17)—N(4)—C(31)	124.98(19)
		C(20)—N(4)—C(31)	109.04(18)
[Cu(L)(DPEphos)](BF$_4$)			
Cu(1)—N(1)	2.041(2)	N(1)—Cu(1)—N(3)	79.33(8)
Cu(1)—N(3)	2.087(2)	N(1)—Cu(1)—P(2)	124.31(6)
Cu(1)—P(1)	2.2743(7)	N(3)—Cu(1)—P(2)	113.73(6)
Cu(1)—P(2)	2.2223(7)	N(1)—Cu(1)—P(1)	110.45(6)
		N(3)—Cu(1)—P(1)	102.45(6)
		P(1)—Cu(1)—P(2)	117.81(3)
[Cu(L)(PPh$_3$)$_2$](BF$_4$)			
Cu(1)—N(1)	2.053(4)	N(1)—Cu(1)—N(3)	79.36(17)
Cu(1)—N(3)	2.094(4)	N(1)—Cu(1)—P(1)	112.88(14)
Cu(1)—P(1)	2.2297(16)	N(3)—Cu(1)—P(1)	116.25(13)
Cu(1)—P(2)	2.2469(16)	N(1)—Cu(1)—P(2)	120.49(13)
Cu(2)—N(5)	2.0310(5)	N(3)—Cu(1)—P(2)	108.72(14)
Cu(2)—N(7)	2.1510(5)	P(1)—Cu(1)—P(2)	114.42(6)
Cu(2)—P(4)	2.2337(15)	N(5)—Cu(2)—N(7)	78.48(18)
Cu(2)—P(3)	2.2502(17)	N(5)—Cu(2)—P(4)	114.34(13)
		N(7)—Cu(2)—P(4)	117.12(13)
		N(5)—Cu(2)—P(3)	117.75(14)
		N(7)—Cu(2)—P(3)	106.34(13)
		P(4)—Cu(2)—P(3)	116.72(6)

Table 1
Crystallographic data for the ligand **L** and the Cu(I) complexes.

Compound	L	[Cu(L)(DPEphos)](BF$_4$) 2CH$_3$CN	[Cu(L)(PPh$_3$)$_2$](BF$_4$)·1/4CH$_3$CH$_2$OCH$_2$CH$_3$
Empirical formula	$C_{31}H_{22}N_4$	$C_{71}H_{56}CuN_6OP_2BF_4$	$C_{68}H_{54.50}CuN_4O_{0.25}P_2BF_4$
Formula weight	450.53	1221.51	1143.95
Temperature (K)	188(2)	185(2)	185(2)
Wavelength (Å)	0.71073	0.71073	0.71073
Crystal system	Monoclinic	Triclinic	Triclinic
Space group	$P2_1/c$	P − 1	P − 1
Unit cell dimensions			
a (Å)	9.4419(8)	13.7645(8)	15.0050(7)
b (Å)	33.1510(3)	13.8050(8)	15.2591(7)
c (Å)	7.7622(6)	17.3552(10)	28.1291(13)
α (°)	90	72.3520(10)	86.5870(10)
β (°)	101.9560(10)	78.8590(10)	78.1700(10)
γ (°)	90	86.0670(10)	78.5480(10)
Volume (Å^3), *Z*	2376.9(3), 4	3083.2(3), 2	6177.0(5), 4
Density (calculated) (g/cm^3)	1.259	1.316,	1.230
Absorption coefficient (mm^{-1})	0.075	0.468	0.461
F(000)	944	1264	2370
Crystal size (mm)	0.28 × 0.21 × 0.14	0.32 × 0.24 × 0.12	0.31 × 0.23 × 0.10
θ Range for data collected (°)	2.20–26.03	1.51–26.02	1.46–25.03
Limiting indices	$-9 \leqslant h \leqslant 11$, $-38 \leqslant k \leqslant 40$, $-9 \leqslant l \leqslant 9$	$-16 \leqslant h \leqslant 16$, $-15 \leqslant k \leqslant 17$, $-15 \leqslant l \leqslant 21$	$-17 \leqslant h \leqslant 16$, $-17 \leqslant k \leqslant 18$, $-33 \leqslant l \leqslant 33$
Reflections collected	14826	19853	34691
Independent reflections	4682 (R_{int} = 0.0333)	11880 (R_{int} = 0.0243)	21488 (R_{int} = 0.00487)
Max. and min. transmission	0.9895 and 0.9792	0.9460 and 0.8647	0.9554 and 0.8703
Data/restraints/parameters	4682/29/316	11880/0/777	21488/7/1469
-fit on F^2	1.017	1.023	1.011
Final *R* indices [$I > 2\sigma(I)$]	R_1 = 0.0596, wR_2 = 0.1385	R_1 = 0.0494, wR_2 = 0.1143	R_1 = 0.0828, wR_2 = 0.2000
R indices (all data)	R_1 = 0.0869, wR_2 = 0.1543	R_1 = 0.0697, wR_2 = 0.1263	R_1 = 0.1317, wR_2 = 0.2282
Largest diff. peak and hole (e Å^{-3})	0.787 and −0.238	0.742 and −0.371	1.258 and −0.524

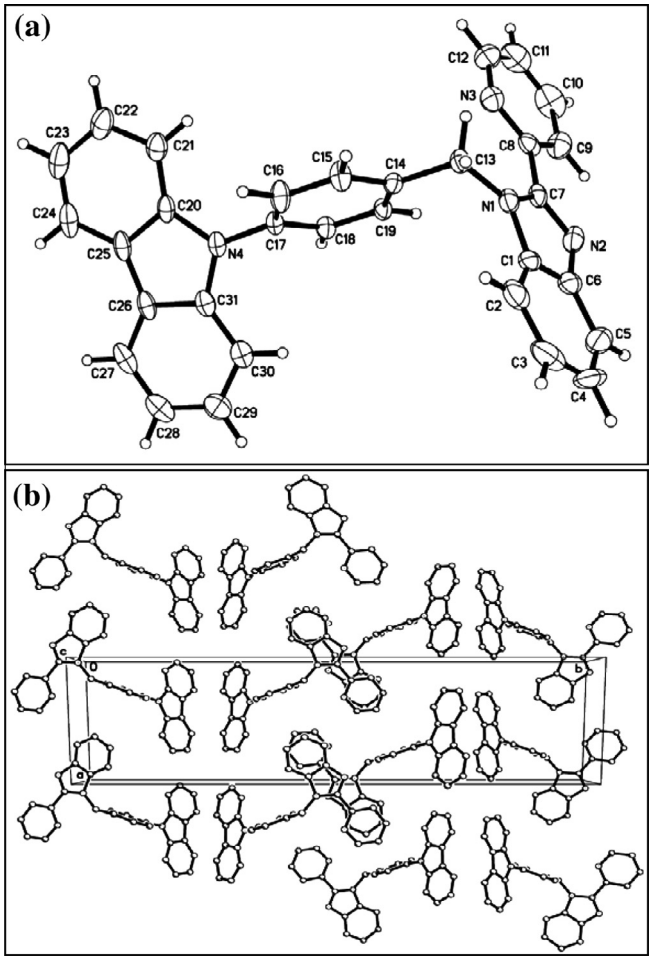

Fig. 1. Crystal structure (a) and packing diagram (b) of the ligand **L**.

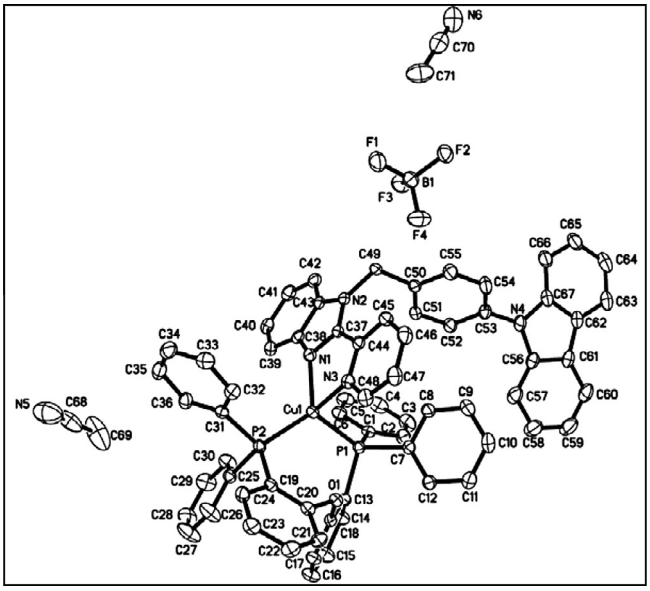

Fig. 2. Crystal structure of complex $[Cu(L)(DPEphos)](BF_4)$. Hydrogen atoms are removed for clarity.

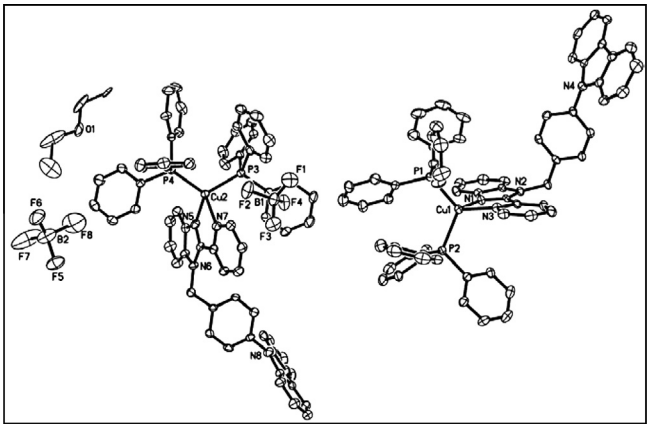

Fig. 3. Crystal structure of complex $[Cu(L)(PPh_3)_2](BF_4)$. Hydrogen atoms are removed for clarity.

the Cu(I) complexes, they are all yellow crystals. The crystals of the Cu(I) complexes suitable for X-ray analysis were obtained as the solvate species $[Cu(L)(DPEphos)](BF_4)\cdot 2CH_3CN$ and $[Cu(L)(PPh_3)_2](BF_4)\cdot 1/4CH_3CH_2OCH_2CH_3$, whose crystal structures are given in Figs. 2 and 3, respectively. Their crystal data and experimental details are shown in Table 1, and the selected bond lengths and angles are listed in Table 2.

The crystal structure of $[Cu(L)(DPEphos)](BF_4)\cdot 2CH_3CN$ comprises of a $[Cu(L)(DPEphos)](BF_4)$ molecule and two crystallizing acetonitrile molecules. The crystal of $[Cu(L)(DPEphos)](BF_4)$ belongs to the triclinic space group $P-1$, $a = 13.7645(8)$ Å, $b = 13.8050(8)$ Å, $c = 17.3552(10)$ Å, $\alpha = 72.3520(10)°$, $\beta = 78.8590(10)°$, $\gamma = 86.0670(10)°$, $U = 3083.2(3)$ Å^3, $Z = 2$, $D_c = 1.316$ g cm^{-3}, $\mu = 0.468$ mm^{-1}. As shown in Fig. 2, the coordination center of Cu atom is surrounded by two N atoms from **L** ligand and two P atoms from the ancillary ligand DPEphos. From the key geometric parameters shown in Table 1, the coordination sphere around Cu(I) center is identified as a distorted tetrahedral one. The intersection angle of N—Cu—N and P—Cu—P planes is as large as 88.74°, and this large intersection angle suggests that the coordination environment around Cu(I) center is highly crowded. The two Cu—P bond lengths are 2.2223(7) and 2.2743(7) Å, respectively, indicating that the coordination abilities of two P atoms from DPEphos are different due to the structural distortion of DPEphos ligand. The Cu(1)—N(3) (pyridyl) bond length (2.087(2) Å) is longer than the Cu(1)—N(1) (imidazolyl) bond length (2.041(3) Å), which means that the intermolecular attraction between Cu(I) center and N (imidazolyl) is stronger than that between Cu(I) center and N (pyridyl). The N—Cu—N and P—Cu—P bond angles are 79.33(8) and 117.81(3), respectively. The unbound ether oxygen of the DPEphos ligand lies at a distance of 3.126 Å from the Cu(I) center and opposite that of N(1) [N(1)—Cu(1)—O(1) = 168.54°]. Similar Cu—O separations were also observed in DPEphos Cu (I) complexes that containing 1,10-phenanthroline derivative ligands [21] and 2-(2-pyridyl)benzimidazolyl derivative ligands [27], but the Cu—O distance and the angle of N(1)—Cu(1)—O(1) in the complex $[Cu(L)(DPEphos)](BF_4)$ are all smaller than those reported in the literatures.

In the chelated ligand **L**, the pyridyl ring is not coplanar with the benzimidazolyl ring, the dihedral angle between them is 9.29°, which is larger than that in the free ligand **L** (0.55°). It is indicated that the plane of pyridyl group and the plane of benzimidazole ring takes place slight distortion due to coordination of two N atoms to the Cu center atom.

The packing diagram of the complex $[Cu(L)(PPh_3)_2](BF_4)$ crystal is shown in Fig. 4. In one unit cell, there are two $[Cu(L)(PPh_3)_2](BF_4)$ molecules, and there is a anti-parallel interaction between the benzimidazole rings of the two $[Cu(L)(PPh_3)_2](BF_4)$ molecules, the interplanar distance is approximately 3.29 Å, which means a strong intermolecular π–π stacking interaction between cations of $[Cu(L)(PPh_3)_2](BF_4)$.

Fig. 3 gives the crystal structure of complex $[Cu(L)(PPh_3)_2](BF_4)$. It indicates that the asymmetric unit of complex $[Cu(L)(PPh_3)_2](BF_4)$ consists of two crystallographic-separate complexes and half of diethyl ether molecule. Thus, the crystal of the Cu(I) complex suitable for X-ray analysis was described as the solvate species $[Cu(L)(PPh_3)_2](BF_4)\cdot 1/4CH_3CH_2OCH_2CH_3$. Its crystal also belongs to the triclinic space group $P-1$, $a = 15.0050(7)$ Å, $b = 15.2591(7)$ Å, $c = 28.1291(13)$ Å, $\alpha = 86.5870(10)°$, $\beta = 78.1700(10)°$, $\gamma = 78.5480(10)°$, $U = 6177.0(5)$ Å^3, $Z = 4$, $D_c = 1.230$ g cm^{-3}, $\mu = 0.461$ mm^{-1}. The coordination center of Cu atom is tetracoordinated by two N atoms from **L** ligand and two P atoms from two PPh_3 ligands, displaying distorted tetrahedral coordination geometry. The two Cu—P bond lengths are 2.2297(16) and 2.2469(16) Å, respectively. The Cu(1)—N(3) (pyridyl) bond length (2.0940(4) Å) is longer than the Cu(1)—N(1) (imidazolyl) bond length (2.0530(4) Å). The intersection angle of N—Cu—N and P—Cu—P planes is as large as 83.60°. The N—Cu—N and P—Cu—P bond angles are 79.36(17) and 114.42(6), respectively.

For the chelated ligand **L** in the crystal, the pyridyl ring is not coplanar with the benzimidazolyl ring, the dihedral angle between them is 6.12°, indicating that the plane of pyridyl group and the plane of benzimidazole ring takes place slight distortion due to coordination of two N atoms to the Cu center atom.

In addition, owing to highly disordered effect of the phenyl rings of PPh_3 ligands and steric hindrance of carbazole group of ligand **L**, there is no inter- or inner-molecular π–π stacking interaction in the crystal lattice.

UV–vis absorption and photoluminescence of the Cu(I) complexes

The UV–vis absorption spectra of dilute dichloromethane solutions of the Cu (I) complexes and the free ligands are shown in Fig. 5. The absorption spectra of free DPEphos and PPh_3 are similar, exhibiting two absorption bands at 234 and 260 nm. The free ligand **L** has three intensive absorption bands at 241, 294 and 312 nm, respectively. The absorption spectra of the complexes $[Cu(L)(DPEphos)](BF_4)$ and $[Cu(L)(PPh_3)_2](BF_4)$ strongly resemble each other, which can be described as two components: an intense absorption region in high energy region ranging from 220 to 360 nm and a weak absorption region in low energy region ranging from 360 to 480 nm. In intense absorption region, there are five visible absorption peaks at 228, 283, 294, 325 and 340 nm. Comparing with the absorption spectra of free ligands, the high energy absorption bands of the complexes are found to be quite similar to those of free ligands and thus attributed to the $\pi \rightarrow \pi^*$ transitions of the ligands. The weak absorption band of the complex

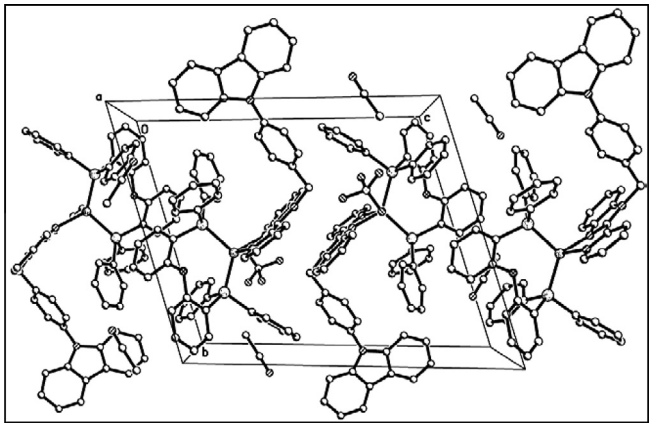

Fig. 4. Three-dimensional packing diagram of the complex $[Cu(L)(PPh_3)_2](BF_4)$ crystal. Hydrogen atoms are removed for clarity.

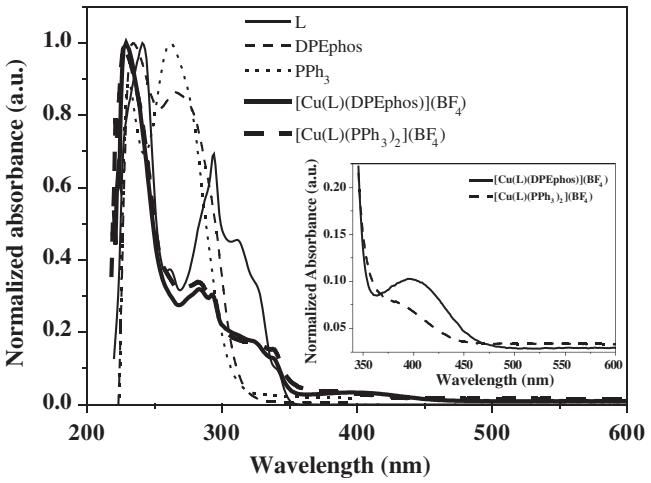

Fig. 5. Absorption spectra of free ligands and the Cu(I) complexes in dichloromethane solutions at room temperature. The inset shows a magnified view of the absorption edges for the Cu(I) complexes ($C = 1 \times 10^{-5}$ mol/L).

$[Cu(L)(DPEphos)](BF_4)$ or $[Cu(L)(PPh_3)_2](BF_4)$, which is a newly generated one compared with those of free ligands, is characteristic of metal-to-ligand charge-transfer (MLCT) transitions [27,28].

Fig. 6 shows the photoluminescent spectra of the Cu(I) complexes powders upon excitation wavelength of 400 nm measured at 298 K. The photoluminescence spectra of the complexes $[Cu(L)(DPEphos)](BF_4)$ and $[Cu(L)(PPh_3)_2](BF_4)$ strongly resemble each other, they all exhibit strong orange emission. The complexes display single broad emission bands with $\lambda_{max} = 605$ and 614 nm, respectively, which are assigned to the $d\pi(Cu) \rightarrow \pi^*$(diimine) (^{3}MLCT) excited state [13,29]. The broad emission bands have a full width at half maximum (FWHM) of 138 nm, showing no vibronic progressions, and the result shows that the emissive states have a charge-transfer character [30]. The Stokes shift ($\Delta\bar{U}$) between the longest absorption edge (473 nm for $[Cu(L)(DPEphos)](BF_4)$ and 460 nm for $[Cu(L)(PPh_3)_2](BF_4)$) and emission peak (605 nm for $[Cu(L)(DPEphos)](BF_4)$ and 614 nm for $[Cu(L)(PPh_3)_2](BF_4)$) is calculated to be as large as 4612.7 cm^{-1} and 5452.5 cm^{-1}, respectively, which suggests an intense structural distortion occurs in the excited state of $[Cu(L)(DPEphos)](BF_4)$ and $[Cu(L)(PPh_3)_2](BF_4)$. The Stokes shift ($\Delta\bar{U}$) of $[Cu(L)(PPh_3)_2](BF_4)$ is larger than that of $[Cu(L)(DPEphos)](BF_4)$, it seems that DPEphos ligand cannot fully

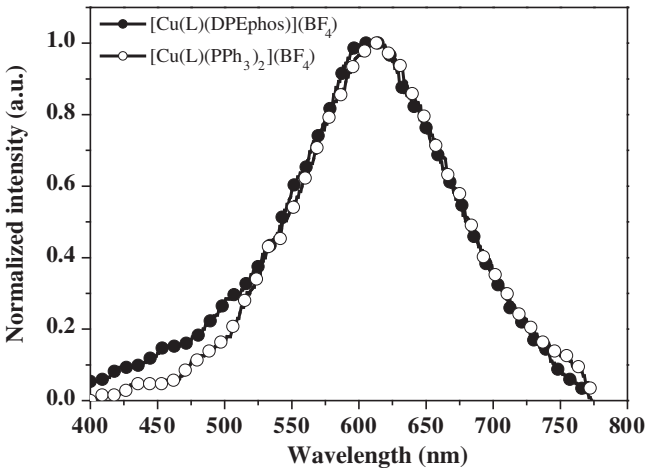

Fig. 6. Photoluminescent spectra of $[Cu(L)(DPEphos)](BF_4)$ and $[Cu(L)(PPh_3)_2](BF_4)$ powders at room temperature.

suppress the structural distortion due to the restricting effect of O atom [31].

However, at room temperature, [Cu(L)(DPEphos)](BF_4) and [Cu(L)(PPh_3)$_2$](BF_4) do not display any detectable emission in air-saturated dichloromethane solutions, clearly indicating the triplet nature of the emission.

Conclusions

A new 2-(2′-pyridyl)benzimidazole ligand (**L**) in which 2-(2′-pyridyl)benzimidazole is linked to a 4-(9*H*-carbazol-9-yl)phenyl fluorophore by a methylene spacer and two new mononuclear Cu(I) complexes containing hole-transporting carbazoly moiety, [Cu(L)(DPEphos)](BF_4) and [Cu(L)(PPh_3)$_2$](BF_4), were synthesized and characterized by elemental analysis, ^{1}H NMR and single crystal X-ray crystallography. The single crystal X-ray diffraction study of the Cu(I) complexes reveal that the center Cu(I) ion assumes highly distorted tetrahedral geometry. All the complexes exhibit strong orange emission in the solid state at room temperature assigned to $d\pi$(Cu) → π^*(diimine) (^{3}MLCT) transitions.

Supplementary material

CCDC 898315, 898316 and 898317 contain the supplementary crystallographic data for ligand **L**, [Cu(L)(DPEphos)](BF_4)·2CH_3CN and [Cu(L)(PPh_3)$_2$](BF_4)·1/4$CH_3CH_2OCH_2CH_3$. These data can be obtained free of charge via http://www.ccdc.cam.ac.uk/conts/retrieving.html, or from the Cambridge Crystallographic Data Center, 12 Union Road, Cambridge CB2 1EZ, UK; fax: +44 1223 336 033; or e-mail: deposit@ccdc.cam.ac.uk.

Acknowledgements

This work was supported by the Science and Technology Project of Lanzhou (2009-1-15), and also supported by the Program for Changjiang Scholars and Innovative Research Team in University (IRT0629).

References

[1] L.X. Xiao, Z.J. Chen, B. Qu, J.X. Luo, S. Kong, Q.H. Gong, J. Kido, Adv. Mater. 23 (2011) 926–952.
[2] Z.M. Hudson, C. Sun, M.G. Helander, H. Amarne, Z.H. Lu, S. Wang, Adv. Funct. Mater. 20 (2010) 3426–3439.
[3] C. Borek, K. Hanson, P.I. Djurovich, M.E. Aznavour, R. Bau, Y. Sun, S.R. Forrest, J. Brooks, L. Michalski, J. Brown, Angew. Chem. Int. Ed. 46 (2007) 1109–1112.
[4] C. Wu, H.F. Chen, K.T. Wong, M.E. Thompson, J. Am. Chem. Soc. 132 (2010) 3133–3139.
[5] A. Kapturkiewicz, Electrochemiluminescent systems as devices and sensors. In electrochemistry of functional supramolecular systems, in: P. Ceroni, A. Credi, M. Venturi (Eds.), John Wiley & Sons, Hoboken, NJ, 2010.
[6] K.K.W. Lo, M.W. Louie, K.Y. Zhang, Coord. Chem. Rev. 254 (2010) 2603–2622.
[7] Q. Zhao, F.Y. Li, C.H. Huang, Chem. Soc. Rev. 39 (2010) 3007–3030.
[8] M.X. Yu, Q. Zhao, L.X. Shi, F.Y. Li, Z.G. Zhou, H. Yang, T. Yi, C.H. Huang, Chem. Commun. (2008) 2115–2117.
[9] S.W. Botchway, M. Charnley, J.W. Haycock, A.W. Parker, D.L. Rochester, J.A. Weinstein, J.A. Gareth Williams, Proc. Natl. Acad. Sci. USA 105 (2008) 16071–16076.
[10] M. Thompson, MRS Bull. 32 (2007) 694–701.
[11] M.A. Baldo, D.F. O'Brien, Y. You, A. Shoustikov, S. Sibley, M.E. Thompson, S.R. Forrest, Nature 395 (1998) 151–154.
[12] M.E. Kondakova, T.D. Pawlik, R.H. Young, D.J. Giesen, D.Y. Kondakov, C.T. Brown, J.C. Deaton, J.R. Lenhard, K.P. Klubek, J. Appl. Phys. 104 (2008) 094501–94517.
[13] L.F. Shi, B. Li, Eur. J. Inorg. Chem. 48 (2009) 2294–2302.
[14] Z. Li, Spectrochim. Acta Part A 81 (2011) 475–480.
[15] E.A. Lewis, W.B. Tolman, Chem. Rev. 104 (2004) 1047–1076.
[16] M. Hashimoto, S. Igawa, M. Yashima, I. Kawata, M. Hoshino, M. Osawa, J. Am. Chem. Soc. 133 (2011) 10348–10351.
[17] J.C. Deaton, S.C. Switatski, D.Y. Kondakov, R.H. Young, T.D. Pawlik, D.J. Giesen, S.B. Harkins, A.J.M. Miller, S.F. Mickenberg, J.C. Peters, J. Am. Chem. Soc. 132 (2010) 9499–9508.
[18] L. Zhang, B. Li, Z.M. Su, J. Phys. Chem. C 113 (2009) 13968–13973.
[19] A. Wada, Q.S. Zhang, T. Yasuda, I. Takasu, S. Enomoto, C. Adachi, Chem. Commun. 48 (2012) 5340–5342.
[20] G.J. Kubas, Inorg. Synth. 19 (1979) 90–92.
[21] D.G. Cuttell, S.M. Kuang, P.E. Fanwick, D.R. McMillin, R.A. Walton, J. Am. Chem. Soc. 124 (2002) 6–7.
[22] S.M. Kuang, D.G. Cuttell, D.R. McMillin, P.E. Fanwick, R.A. Walton, Inorg. Chem. 41 (2002) 3313–3322.
[23] B.D. Spangler, C.W. Spangler, E. Scott Tarter, US Patent 0043109 A1, 2009.
[24] P. Rajakumar, N. Venkatesan, K. Sekar, S. Nagaraj, R. Rengasamy, Eur. J. Med. Chem. 45 (2010) 1220–1224.
[25] L. Xu, Z.J. Zhao, Y.J. Xing, P. Lu, J. Zhejiang Univ. Sci. A 9 (2008) 1590–1594.
[26] C.L. Ho, Q. Wang, C.S. Lam, W.Y. Wong, D.G. Ma, L.X. Wang, Z.Q. Gao, C.H. Chen, K.W. Cheah, Z.Y. Lin, Chem. Asian J. 4 (2009) 89–103.
[27] T. McCormick, W.L. Jia, S.N. Wang, Inorg. Chem. 45 (2006) 147–155.
[28] L.M. Zhang, B. Li, Z.M. Su, Langmuir 25 (2009) 2068–2074.
[29] O. Moudam, A. Kaeser, B. Delavaux-Nicot, C. Duhayon, M. Holler, G. Accorsi, N. Armaroli, I. Séguy, J. Navarro, P. Destruel, J. Nierengarten, Chem. Commun. (2007) 3077–3079.
[30] H. Kupka, W. Ensslin, R. Wernicke, H. Schmidtke, Mol. Phys. 37 (1979) 1693–1701.
[31] J.L. Sun, J. Lumin. 132 (2012) 1515–1521.